Scientia Pharmaceutica

ÖSTERREICHISCHE PHARMAZEUTISCHE GESELLSCHAFT

MDPI

Article

The Preservation and Enantiomeric Selection of Linalool by Nanoencapsulation Using Cyclodextrins

Tanaporn Poonphatanapricha, Sasimas Katanyutanon, Kulpavee Jitapunkul, Luckhana Lawtrakul * and Pisanu Toochinda *

School of Bio-Chemical Engineering and Technology (BCET), Sirindhorn International Institute of Technology (SIIT), Thammasat University, Pathum Thani 12120, Thailand; tanaporn.poonphat@gmail.com (T.P.); por.katanyutanon@gmail.com (S.K.); kulpavee.work@gmail.com (K.J.)

* Correspondence: luckhana@siit.tu.ac.th (L.L.); pisanu@siit.tu.ac.th (P.T.); Tel.: +66-2-986-9009 (ext. 2301) (L.L.); +66-2-986-9009 (ext. 2309) (P.T.)

Abstract: Linalool, a volatile terpene alcohol, is responsible for a characteristic aroma in food, beverages, and cosmetics. However, linalool's low aqueous solubility and high volatility limit the applications and shelf life of linalool-containing products. Nanoencapsulation using beta-cyclodextrin (BCD), methyl-beta-cyclodextrin (MBCD) and hydroxypropyl-beta-cyclodextrin (HPBCD) was studied to improve the aqueous solubility and stability of linalool. Linalool has two enantiomers with distinct flavors and odors which affect product quality. The enantiomeric selectivity of the cyclodextrins (CDs) toward racemic linalool standard was evaluated. A computational simulation was performed to predict the conformations and interactions of the inclusion complexes. The 1:1 host-guest ratio from the computer simulation was implemented in the experimental study. Phase solubility study shows an improvement in linalool aqueous solubility after being encapsulated by CDs. The encapsulation efficiencies of linalool/BCD, linalool/MBCD, and linalool/HPBCD inclusion complexes are 66.30%, 51.38% and 32.31%, respectively. Nanoencapsulation by CDs can preserve linalool in the form of inclusion complexes compared to its free form. The amount of remaining linalool in linalool/BCD, linalool/MBCD, and linalool/HPBCD inclusion complexes are 89.57%, 87.07%, and 74.86%, respectively which are considerably larger than that of pure linalool (42.30%). CDs also show the enantiomeric selectivity toward (*R*)-linalool as evident from (*R*)-linalool percentage of 54.53% in the inclusion complex.

Keywords: linalool; stability improvement; enantiomeric selection; inclusion complex; molecular modeling

Citation: Poonphatanapricha, T.; Katanyutanon, S.; Jitapunkul, K.; Lawtrakul, L.; Toochinda, P. The Preservation and Enantiomeric Selection of Linalool by Nanoencapsulation Using Cyclodextrins. *Sci. Pharm.* **2021**, *89*, 42. https://doi.org/10.3390/scipharm89030042

Academic Editors: Roman B. Lesyk and Franz Bracher

Received: 11 July 2021
Accepted: 31 August 2021
Published: 3 September 2021

1. Introduction

Linalool, an unsaturated terpene alcohol from plants, provides a remarkable aroma which is used in several industries such as food, beverage, and cosmetic. Linalool is also utilized for its carcinogenic, antidiabetic, antioxidant, and antimicrobial properties [1]. Commercial products containing linalool may suffer from limited shelf life due to linalool's low aqueous solubility and high volatility [2]. To increase the shelf life of the products and prevent linalool degradation, a nanoencapsulation technique can be utilized to preserve and stabilize linalool. Linalool has two enantiomers which are (*R*)-linalool and (*S*)-linalool. (*R*)-linalool has a woody, lavender-like aroma while (*S*)-linalool has a sweet, floral, herb-like aroma [3]. The two enantiomers have considerably different perception thresholds for humans. (*R*)-linalool has the odor perception of 0.008 ppm in air which is around 10 times lower than that of (*S*)-linalool [4,5]. The difference in linalool enantiomer ratio leads to different taste and odor of linalool-containing products. For example, espresso with (*R*)-linalool has honey, flowery and caramel notes. With a higher ratio of (*S*)-linalool, the flowery note will become intense and overpower the other two notes [6].

An encapsulation technique is used in many applications to stabilize volatile aromatics during product processing and storage and to protect the products from degradation by heat, humidity, or chemical reactions. For essential oil encapsulation, including linalool, widely used host molecules are cyclodextrins (CDs). The structure of CD, which is a truncated cone with hydrophobic inner cavity and hydrophilic outer surface, gives it an ability to encapsulate, stabilize, and enhance the aqueous solubility of guest molecules [7–9]. The possibility of inclusion complex formation depends on the host and guest molecules with the main driving force being an apolar-apolar interaction between the guest molecule and the host's inner cavity [10]. In addition, CDs have an ability to separate the enantiomers of guest molecules due to their asymmetric centers [11,12]. Beta-cyclodextrin (BCD) is a common type of CD used in the pharmaceutical, cosmetic, and food industries due to its safety, cost, and cavity size which is appropriate for common plant compounds [13]. Derivatives of BCD, dimethyl-beta-cyclodextrin (MBCD) and 2-*O*-monohydroxypropyl-beta-cyclodextrin (HPBCD), are also widely used in drug encapsulation due to their aqueous solubility (500 mg/mL) which is more than 20-fold of that of BCD (18.4 mg/mL) [14]. The research from Abril-Sánchez et al. showed the efficacy improvement of the citronellal essential oil after being encapsulated by HPBCD. The encapsulation technique was proven to enhance the solubility and stability of citronellal which was confirmed by GC/MS and sensory analysis [15].

A computational simulation was performed to predict the inclusion complex formation including the host-guest ratio, the interactions, and the conformations of the linalool/CD inclusion complexes. From the fact that linalool has two enantiomers, computational simulation was also used to compare the differences in the interactions, the conformations, and the binding energy of (*R*)-linalool and (*S*)-linalool/CD inclusion complexes to investigate the enantiomeric selection of linalool by CDs. Since there are no experimental studies confirming linalool enantiomeric selection together with the aqueous solubility and stability improvement by an encapsulation technique, this study focused on linalool encapsulation using BCD, MBCD, and HPBCD based on the computational simulation results.

The major objectives of this work are: (1) to investigate linalool/CD inclusion complex formation with computational simulation and verify the results with experimental study, (2) to investigate the aqueous solubility enhancement and the stability improvement of linalool/CD inclusion complexes compared to pure linalool, and (3) to evaluate the enantioselectivity of CDs toward (*R*)- and (*S*)-linalool encapsulation.

2. Materials and Methods

2.1. Computational Simulation of Linalool/CD Inclusion Complex Formation

Discovery Studio 4.0 Visualizer program [16] was used to construct both of *R* and *S* linalool enantiomers and to modify atoms and bonds of BCD, MBCD, and HPBCD which were downloaded from Cambridge Crystallographic Data Centre with identifiers: BCDEXD03 [17], BOYFOK04 [18], and KOYYUS [19], respectively (Figures 1 and 2). All molecules were then fully minimized by semiempirical PM7 calculations via Gaussian16 program package [20]. AutoDock 4.2.6 program [21] with the Lamarckian genetic algorithm were used to simulate the possible conformations of linalool/BCD inclusion complexes. The systems were investigated in three dimensions of 15 Å × 15 Å × 15 Å, with a grid spacing of 0.75 Å. The BCD host molecule was kept fixed while the guest linalool was flexible and free to rotate and move inside the grid volume. One hundred docking calculations were performed, and the results were clustered based on all atoms root-mean-square deviation (RMSD) within 2 Å. A representative docked conformation with lowest Gibbs free energy (ΔG) from molecular docking was selected for further full geometry minimization.

The complexation energy (Δ*E*) of 1:1 molecular ratio between (*R*)-linalool/BCD and (*S*)-linalool/BCD in the minimized geometries are evaluated by Equation (1).

$$\Delta E = E_{\text{complex}} - (E_{\text{host}} + E_{\text{guest}}) \quad (1)$$

where $E_{complex}$, E_{host}, and E_{guest} represent to the heat of formation of the host/guest inclusion complex, the host molecule (BCD), and the guest molecule (linalool) in gas phase, respectively.

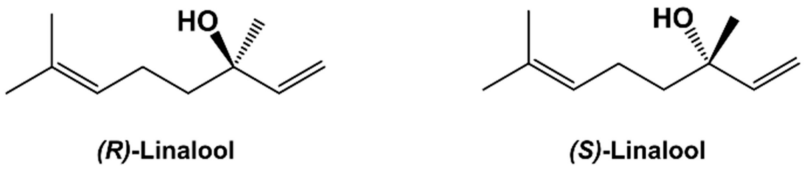

Figure 1. Chemical structure of linalool ((*R*)- and (*S*)-enantiomers).

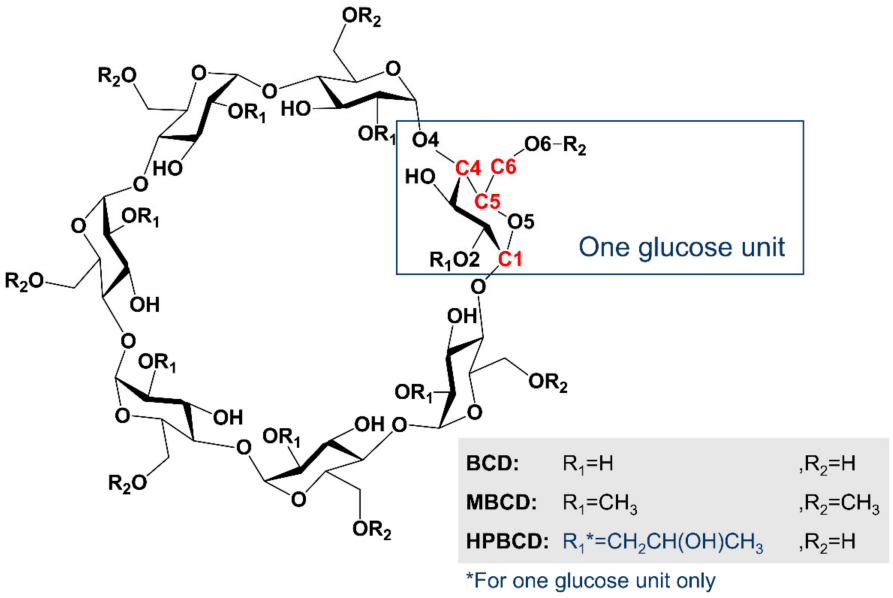

Figure 2. Schematic representation of glucose unit and atomic numbering of BCD, MBCD, and HP-BCD. (C1, C4, C5, and C6 refer to the numeric indexes of carbon atom position in each glucose unit).

The dynamics of the inclusion complexes of BCD with (*R*)-linalool were carried out from the solid-state complex of a 2:2 host-guest stoichiometry which was deposited in Cambridge Crystallographic Data Centre with identifier: UKIXAP [22]. Molecular dynamics simulation (MD) of this complex was performed using AMBER20 program package [23] with GLYCAM-06 [24] and AMBER force fields. The (*R*)-linalool/BCD dimeric complex was solvated in a periodic truncated octahedral box with TIP3P water molecules. Energy minimization was performed with 1000 cycles of steepest descent, followed by 1000 cycles of conjugate gradient, to reduce steric effects between water molecules and the (*R*)-linalool/BCD dimeric complex. Then, the system was gradually heated from 0 to 298.15 K (room temperature) over 100 ps with the volume held constant. Afterwards, the system equilibration was performed using MD simulation for 5 ns with 2 fs time steps under isothermal-isobaric ensemble (NPT) at constant temperature and pressure of 298.15 K and 1 atm, respectively.

2.2. Phase Solubility Study of Linalool/CD Inclusion Complexes

The limited aqueous solubility of linalool may cause it to be poorly distributed in a water-based product. To investigate the change in aqueous solubility of linalool after encapsulation with CDs, the phase solubility study was performed. CD solutions (0–16 mM) were prepared by dissolving solid CDs, which are BCD, MBCD, and HPBCD (Tokyo Chemical Industry, Tokyo, Japan), in RO water. An excess of linalool (97%, Sigma Aldrich, St. Louis, MO, USA) was added to the CD solutions for inclusion complex formation. The

mixtures were shaken in an incubator (BioTek Instruments, Winooski, VT, USA) at 25 °C and 160 rpm for 72 h. Precipitates were filtered out from the mixture. The amount of linalool dissolved in the filtrate was then analyzed by HPLC. Phase solubility diagrams were constructed by plotting the concentrations of linalool dissolved in the filtrate versus the concentrations of CDs.

2.3. Linalool/CD Inclusion Complex Formation

Ethanol is generally used as a co-solvent to improve encapsulation efficiency for various host and guest molecules [25]. In order to obtain the highest encapsulation efficiency, the effect of ethanol concentration on the amount of encapsulated linalool was evaluated. CDs were dissolved in 20 mL of 0 to 80 vol% of ethanol (99.9%, RCI Labscan, Bangkok, Thailand)-water solutions. The solutions were shaken for 3 h. The undissolved CDs were filtered out with filter paper. Linalool was added to each CD solution at 1:1 host-guest molar ratio. The solutions were then shaken in an incubator for 72 h at 25 °C. Linalool/BCD solid complexes that precipitated were filtered and dried in an oven at 60 °C for 72 h. Linalool/MBCD and linalool/HPBCD inclusion complexes did not precipitate, so their solutions were dried in an oven at 60 °C for 72 h to obtain solid inclusion complexes. All the samples were stored at 4 °C.

2.4. Quantitative Analysis of Linalool/CD Inclusion Complexes by High Performance Liquid Chromatography (HPLC)

Quantitative analysis was performed to determine the amount of encapsulated linalool. The obtained solid inclusion complexes were rinsed with cold ethanol (4 °C) and filtered with filter paper to remove free linalool. Linalool/BCD inclusion complex needs to be sonicated at 40 °C for 45 min while linalool/MBCD and linalool/HPBCD needs to be sonicated for 5 min in an ultrasonic sonicator (Crest Ultrasonics, Trenton, NJ, USA). The amount of extracted linalool was quantified by HPLC. Before the injection, all samples were filtered with 0.22-µm syringe filter. The samples were injected to 1260 Infinity II LC system (Agilent Technologies, Santa Clara, CA, USA) equipped with C18 column (Luna 5 µm C18(2) 100 Å, 250 mm × 4.6 mm column, Phenomenex, Torrance, CA, USA). The column temperature was set at 25 °C. The mobile phase was 55% acetonitrile (99.9%, RCI Labscan, Bangkok, Thailand) in type I deionized water (prepared by Milli-Q water purifier, Merck, Burlington, MA, USA) at a flow rate of 1 mL/min. The injection volume was 5 µL. The UV detection wavelength was set at 215 nm with detector sensitivity at 0.005 a.u.f.s and chart speed of 5 mm/min. The amount of encapsulated linalool is represented with the encapsulation efficiency calculated using Equation (2).

$$\text{Encapsulation efficiency } (\%) = \frac{\text{Amount of linalool encapsulated } \times 100}{\text{Amount of linalool initially added}} \quad (2)$$

2.5. Characterization of Linalool/CD Inclusion Complexes by Fourier-Transform Infrared Spectroscopy (FTIR)

FTIR spectrometer (Thermo Fisher Scientific, Waltham, MA, USA) was used to investigate the functional groups of all compounds. FTIR solid samples, i.e., inclusion complexes and pure CDs, were analyzed in the transmission mode using KBr as background. For pure linalool which is in liquid form, the attenuated total reflection (ATR) mode was used. The spectrograms of all samples were recorded at wavenumbers between 400 cm^{-1} and 4000 cm^{-1} with 32 scans and a resolution of 4 cm^{-1}.

2.6. Characterization of Linalool/CD Inclusion Complexes by Thermogravimetric Analysis (TGA)

Thermal analysis of all compounds was performed in TGA (TGA/DSC 1, Mettler-Toledo, Columbus, OH, USA) for mass loss observation with increasing temperature to confirm the inclusion complex formation between linalool and CDs. All samples were weighed and placed in aluminum crucibles and heated from 25 °C to 300 °C at 10 °C/min under nitrogen atmosphere with 20 mL/min flow rate. The thermogravimetric (TG) and

derivative thermogravimetric (DTG) curves of pure linalool, pure CDs, and inclusion complexes were recorded.

2.7. Characterization of Linalool/CD Inclusion Complexes by Differential Scanning Calorimetry (DSC)

The change in energy of compounds with increasing temperature was investigated by DSC (DSC 3+, Mettler-Toledo, Columbus, OH, USA) to confirm the inclusion complex formation between linalool and CDs. All samples were weighed and placed in aluminum crucibles and heated from 25 °C to 450 °C at 10 °C/min under nitrogen atmosphere with 20 mL/min flow rate. The DSC curves of pure linalool, pure CDs and inclusion complexes were recorded.

2.8. Enantiomeric Analysis of Linalool/CD Inclusion Complexes by Gas Chromatography with Flame Ionization Detection (GC-FID)

The enantiomeric selectivity of CDs to separate linalool enantiomers was evaluated. The encapsulated linalool was extracted with ethanol and analyzed with GC-FID (Clarus 580, PerkinElmer, Waltham, MA, USA) equipped with chiral capillary column (MEGA-DEX DET BETA (30 m × 0.32 mm, 0.25 µm film thickness). Before the injection, all samples were filtered with 0.22-µm syringe filter. The injection volume was 1 µL with a split flow of 60, and the temperature was 250 °C. The oven temperature was ramped from 60 °C to 100 °C with the rate of 2 °C/min and from 100 °C to 200 °C with the rate of 30 °C/min, then held for 2 min. The detector temperature was 250 °C. The carrier gas was helium with a flow of 1 mL/min.

2.9. Preservation Study of Linalool/CD Inclusion Complexes

The preservation of linalool in the form of linalool/CD inclusion complexes was evaluated at particular storage conditions i.e., 1 atm and no light with varied storage durations (0–28 days) compared to pure linalool to investigate the stability improvement of linalool after being encapsulated. Ten milligrams of each sample, i.e., inclusion complexes and pure linalool, were stored separately in the incubator at 25 °C for 28 days. The remaining linalool from inclusion complexes was extracted out by ethanol every 7 days and quantified by HPLC. The percentages of the remaining linalool were calculated with Equation (3) and compared between the inclusion complexes and pure linalool.

$$\text{Remaining linalool } (\%) = \frac{\text{Amount of linalool from that day } \times 100}{\text{Amount of linalool from the first day}} \quad (3)$$

3. Results

3.1. Computational Simulation of Linalool/BCD Inclusion Complex Formation

The molecular docking calculations suggest four clusters of linalool/BCD inclusion complexes of both *R* and *S* enantiomers, as presented in Table 1. The structure of BCD (host molecule) is kept fixed while linalool (guest molecule) could freely move inside the grid space in docking simulations. Therefore, further full minimization of host and guest molecules by semiempirical PM7 is necessary. The minimized energy of the representative docked conformation from each cluster is presented in Table 2, and their conformations are represented in Figures 3 and 4 for (*R*)- and (*S*)-linalool inclusion complexes with BCD, respectively.

The structure of BCD has a narrow rim containing the primary 6-hydroxyl groups of the glucose molecules, while the wider rim is formed by the secondary 2- and 3-hydroxyl groups. The calculation results indicate two possible orientations of 1:1 host-guest stoichiometry of the linalool enantiomer inclusion complex with BCD in gas-state. The first orientation (Orientation-I) is found in cluster (1), (2), and (3), and the other (Orientation-II) is found in cluster (4).

Table 1. The lowest and the average Gibbs free energy (ΔG) of linalool/BCD, linalool/MBCD, and linalool/HPBCD inclusion complexes and the number of conformations in a cluster (frequency) obtained from molecular docking calculations.

	Cluster	Orientation	Frequency (%)	ΔG (kcal/mol)	
				Lowest	Average
(*R*)-linalool/BCD	(1)	I	64	−4.13	−4.03
	(2)	I	31	−4.10	−4.01
	(3)	I	1	−3.95	−3.95
	(4)	II	4	−3.93	−3.90
(*S*)-linalool/BCD	(1)	I	41	−4.14	−4.01
	(2)	I	46	−4.06	−3.98
	(3)	I	12	−4.04	−3.96
	(4)	II	1	−3.90	−3.90
(*R*)-linalool/MBCD	(1)	I	90	−5.02	−4.86
	(2)	I	6	−4.83	−4.75
	(3)	I	4	−4.60	−4.55
(*S*)-linalool/MBCD	(1)	I	87	−4.98	−4.79
	(2)	I	13	−4.78	−4.71
(*R*)-linalool/HPBCD	(1)	I	69	−4.36	−4.23
	(2)	I	22	−4.30	−4.23
	(3)	I	9	−4.18	−4.06
(*S*)-linalool/HPBCD	(1)	I	86	−4.37	−4.21
	(2)	I	9	−4.28	−4.21
	(3)	II	5	−4.04	−4.00

Table 2. Heat of formation energy (*E*), complexation energy (Δ*E*), and the dipole moment (μ) of the minimized linalool/BCD inclusion complexes structures from PM7 method.

	Orientation	*E* (kcal/mol)	Δ*E* (kcal/mol)	μ (Debye)
Isolated molecule				
(*R*)-linalool		−57.56		1.79
(*S*)-linalool		−57.49		2.16
BCD		−1608.18		7.25
MBCD		−1551.01		1.55
HPBCD		−1664.45		5.82
Inclusion complex (cluster)				
(*R*)-linalool/BCD (1)	I	−1709.68	−43.94	8.48
(*R*)-linalool/BCD (2)	I	−1706.45	−40.71	7.89
(*R*)-linalool/BCD (3)	I	−1707.58	−41.84	8.57
(*R*)-linalool/BCD (4)	II	−1703.56	−37.82	5.19
(*S*)-linalool/BCD (1)	I	−1705.13	−39.46	7.27
(*S*)-linalool/BCD (2)	I	−1710.54	−44.86	7.74
(*S*)-linalool/BCD (3)	I	−1707.42	−41.75	7.08
(*S*)-linalool/BCD (4)	II	−1709.34	−43.67	3.60
(*R*)-linalool/MBCD (1)	I	−1651.99	−43.42	3.23
(*R*)-linalool/MBCD (2)	I	−1652.27	−43.70	4.51
(*R*)-linalool/MBCD (3)	I	−1646.51	−37.94	3.56
(*S*)-linalool/MBCD (1)	I	−1650.41	−41.91	1.79
(*S*)-linalool/MBCD (2)	I	−1649.73	−41.23	4.72
(*R*)-linalool/HPBCD (1)	I	−1765.59	−43.59	2.85
(*R*)-linalool/HPBCD (2)	I	−1771.94	−49.93	8.47
(*R*)-linalool/HPBCD (3)	I	−1759.36	−37.35	6.07
(*S*)-linalool/HPBCD (1)	I	−1763.53	−41.59	7.70
(*S*)-linalool/HPBCD (2)	I	−1765.72	−43.78	5.16
(*S*)-linalool/HPBCD (3)	II	−1764.89	−42.95	4.62

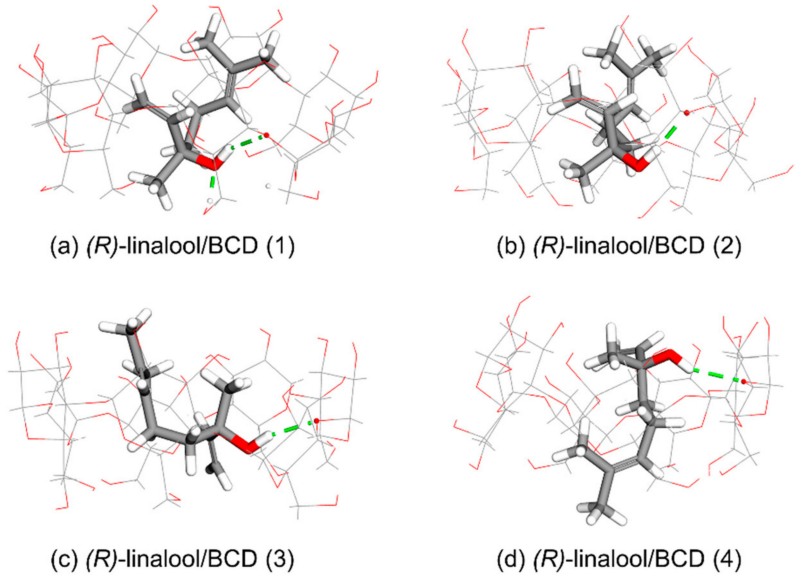

Figure 3. Energy-minimized structure of the 1:1 (*R*)-linalool/BCD complexes from four clusters using PM7 method. BCD is presented as a line model. The linalool molecule is presented as a stick model. The green dashed line refers to hydrogen bond.

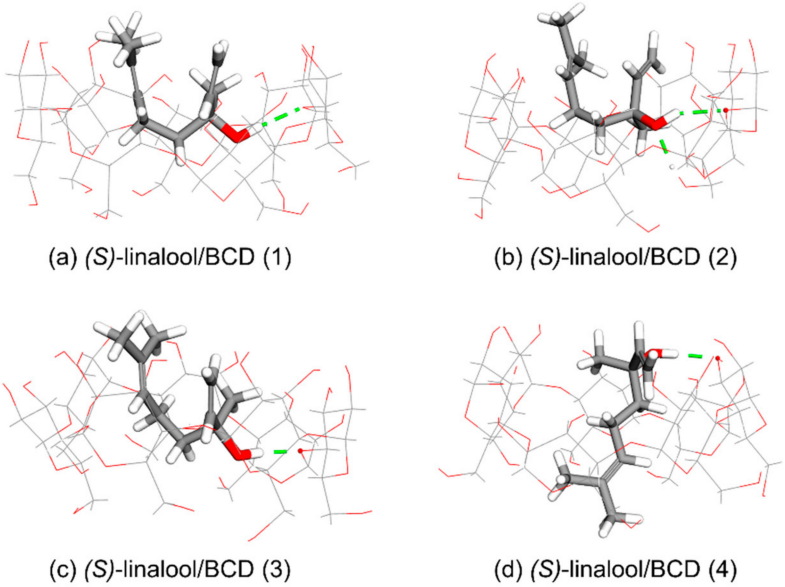

Figure 4. Energy-minimized structure of the 1:1 (*S*)-linalool/BCD complexes from four clusters using PM7 method. BCD is presented as a line model. The linalool molecule is presented as a stick model. The green dashed line refers to hydrogen bond.

Orientation-I, as shown in Figure 3a–c, illustrates the puckering of linalool molecule in which its dimethyl groups is located at the wider rim of BCD while its hydroxyl group points downward inside the BCD's cavity then its methyl group and/or viny group turns upward in the direction to the wider rim of BCD in three different circumstances as follows. In Case 1 which occurs in (*R*)-linalool/BCD (1), (*R*)-linalool/BCD (2), and (*S*)-linalool/BCD (2) complexes, the vinyl group of linalool turns upward to the wider rim while the methyl group is located at the narrow rim, as shown in Figure 3a,b and Figure 4b. In Case 2, the methyl group of linalool turns upward to the wider rim while its vinyl group points downward to the narrow rim, which occurs only in (*R*)-linalool/BCD (3) complex (Figure 3c). Case 3 occurs in (*S*)-linalool/BCD (1), and (*S*)-linalool/BCD (3) complexes,

where both methyl and vinyl groups point upward to the wider rim of BCD, as shown in Figure 4a,c.

Orientation-II, which arises in (*R*)-linalool/BCD (4) and (*S*)-linalool/BCD (4) complexes, illustrates the dimethyl groups of linalool located at the narrow rim of BCD along with its hydroxyl, methyl, and vinyl groups elongated to the wider rim of BCD, as shown in Figures 3d and 4d. In the second orientation, the bond dipoles of linalool molecule cancel each other, yielding a small net molecular dipole. The dipole moment of (*R*)-linalool/BCD (4) and (*S*)-linalool/BCD (4) are 5.19 and 3.60 Debye, while other clusters have the dipole moment between 7.08 and 8.57 Debye (Table 2).

The most stable conformation can be determined based on Gibbs free energy (ΔG) and the complexation energy (Δ*E*) which are inverse variations. In other words, the conformation with the lowest energies is the most stable one. Therefore, as shown in Tables 1 and 2, Orientation-I of (*R*)-linalool/BCD inclusion complex provided the lowest ΔG and Δ*E* of −4.13 and −43.94 kcal/mol, respectively. Orientation-I of (*S*)-linalool/BCD provided the lowest ΔG and Δ*E* of −4.14 and −44.86 kcal/mol, respectively. Consequently, the most stable conformation of (*R*)- and (*S*)-linalool/BCD inclusion complexes is Orientation-I.

Solid-state analysis of the inclusion complexes of BCD with (*R*)-linalool forms the complex of a 2:2 host-guest stoichiometry [22]. The downloaded crystal structure is presented in Figure 5.

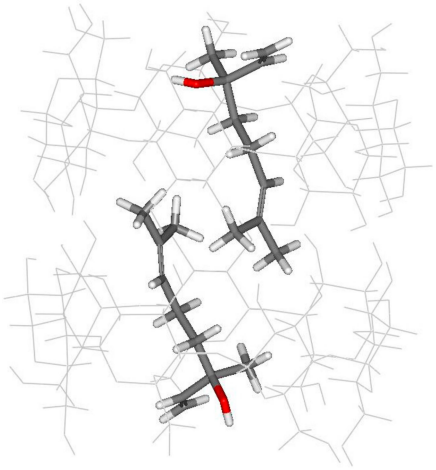

Figure 5. The crystal structure of (*R*)-linalool/BCD [2:2] dimeric complex (UKIXAP). BCD molecules are presented as line models. Linalool molecules are presented as stick models.

The alignment of two linalool molecules inside the head-to-head BCD dimer results in a 2:2 stoichiometry of the formed complex in solid-state. Guest molecules are oriented in head-to-tail mode, with hydroxyl groups pointing toward the narrow rim and their dimethyl groups stretched toward the interface of BCD dimer [22]. There is no interaction between two linalool molecules in the crystal structure. The structure of guest molecules inside each cavity of BCD dimer in solid-state is similar to the structure of 1:1 (*R*)-linalool/BCD Orientation-I in gas-state. Whereas the dimethyl groups are located at the wider rim and its hydroxyl, methyl, and vinyl groups point downward to the narrow rim, resulting from the repulsion of the dimethyl groups from the other linalool molecule.

In order to further investigate the behavior of (*R*)-linalool/BCD dimeric complex in aqueous solution which should represent the possibility of forming 2:2 inclusion complex during the encapsulation process, molecular dynamic simulation (MD) was performed. The RMSD of BCD dimer and (*R*)-linalool molecules have also been observed to determine the stability of the complex as shown in Figure 6. As a result, during 1.75 ns to 2.50 ns, the structures of BCD dimer drastically deviate from the reference structure (at 0 ns), then they are stable for the next few nanoseconds and start to deviate again after 4.25 ns. On the other hand, the structural movement of (*R*)-linalool molecules throughout the simulation

is rather stable. Therefore, this indicated that the dynamic of BCD structures might play an important role in encapsulation of (*R*)-linalool in an aqueous solution.

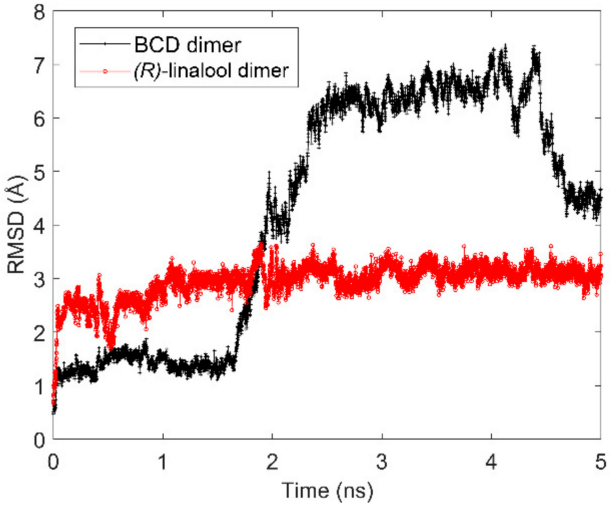

Figure 6. RMSD plot of (*R*)-linalool/BCD dimeric complex during 5 ns of MD simulation.

The dynamic of (*R*)-linalool/BCD dimeric complex was fully investigated from extracted frames during the MD simulation as presented in Figure 7. The BCD dimer was originally connected to each other through hydrogen bonding between hydroxyl groups on the wider rim interface. The dimethyl group of (*R*)-linalool dimer was attracted to each other at the beginning of the simulation (0 ns to 1.5 ns) which resulted in attraction between BCD dimer as well. However, when the (*R*)-linalool dimers were too close to each other as illustrated in a snapshot at 2 ns, the BCD dimer would start to repel each other on one side which resulted in some hydrogen bond breaking. Eventually, it lost the perfect original dimeric form at 2.5 ns snapshot. This is consistent with RMSD result which shows the highest deviation of BCD dimer structure at 2.5 ns. Interestingly, even when the dimeric complex is losing its original form, it is still able to cling onto each other by a few hydrogen bonds. This could also be a result of the weak intermolecular attraction between dimethyl groups of (*R*)-linalool dimer or between the dimethyl group of (*R*)-linalool and adjacent BCD.

Consequently, the binding affinity between (*R*)-linalool dimer and BCD dimer between 3 and 5 ns were investigated in order to determine the efficiency of (*R*)-linalool/BCD encapsulation in the dimeric form. The average binding energy (ΔH) and Gibbs free energy ($\Delta G_{bind)}$ which include the entropy contribution (TΔS) were calculated using MM/GBSA method with 2000 frames from 3 to 5 ns interval as listed in Table 3.

Table 3. Binding energies of (*R*)-linalool dimer and BCD dimer from MM/GBSA calculation.

Component	Energy (kcal/mol)
Average binding energy (ΔH)	−33.58 ± 2.55
Entropy (TΔS at 298.15 K)	−19.12
Gibbs free energy (ΔG_{bind})	−14.46

The negative average binding energy and Gibbs free energy indicated the favorable formation of (*R*)-linalool/BCD dimeric complex. Moreover, the negative entropy could support the immobility of (*R*)-linalool dimer which is trapped inside the cavity of BCD dimer. The average binding energy decomposition between glucose units of BCD and (*R*)-linalool molecules was used to investigate the major intermolecular interactions. As expected, the van der Waals contribution is the highest in each single complex unit of dimeric structure which represents the hydrophobic interaction between (*R*)-linalool molecule and

each glucose unit of BCD. Moreover, the binding interaction between (*R*)-linalool molecule and some glucose units of adjacent BCD are considerably strong (ranging from −2.81 to −0.79 kcal/mol). Thus, this result supports one of the earlier hypotheses that the dimeric structure was held together due to the interaction between (*R*)-linalool and adjacent BCD.

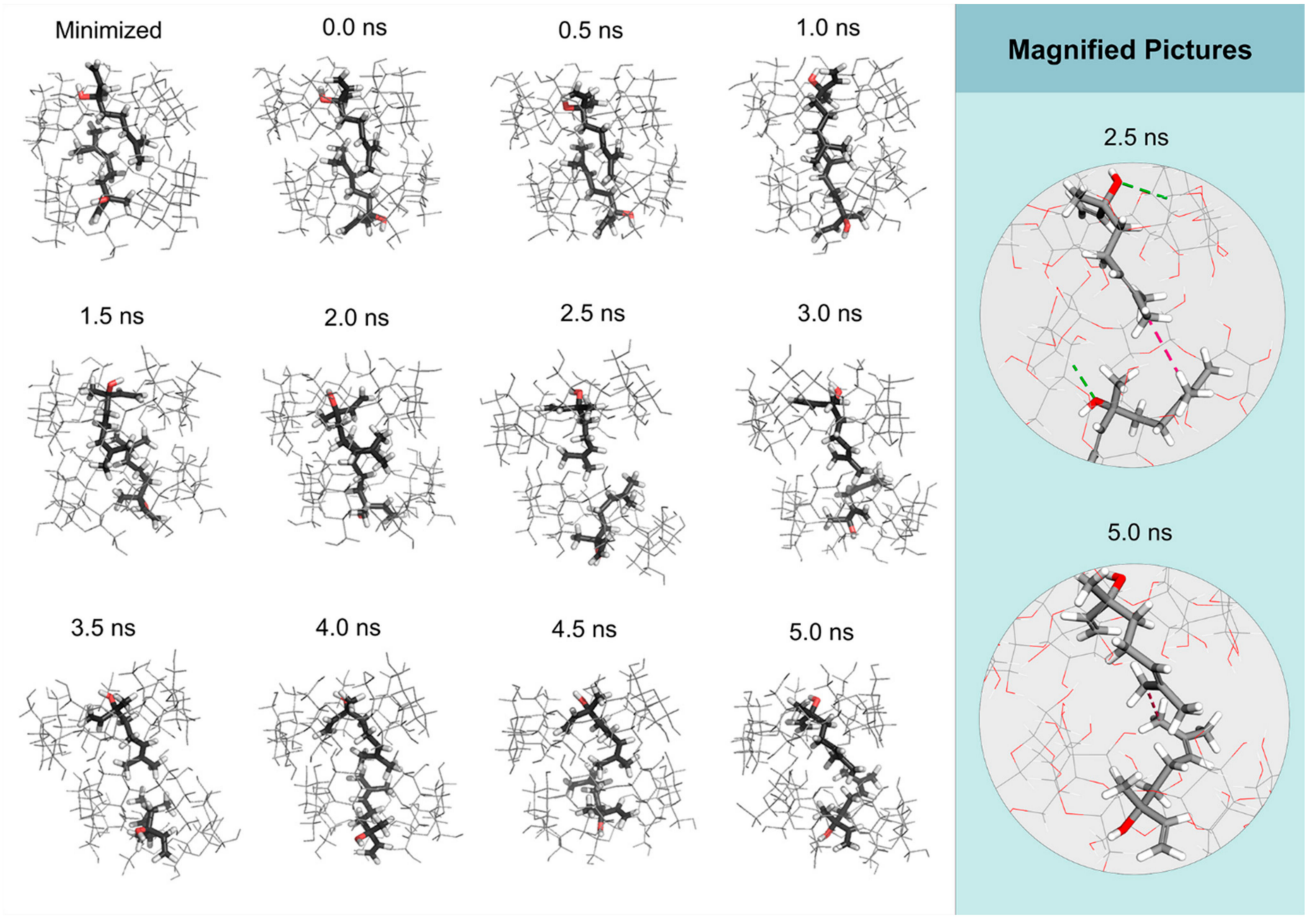

Figure 7. The MD snapshots of (*R*)-linalool/BCD dimeric complex. BCD molecules are presented as line models. Linalool molecules are presented as stick models. The magnified picture of 2.5 and 5 ns snapshot are illustrated on the right to show the intermolecular bonding. The green and pink dashed lines refer to hydrogen bond and hydrophobic interaction, respectively.

3.2. Computational Simulation of Linalool/MBCD Inclusion Complex

Three clusters of docking results are obtained for (*R*)-linalool/MBCD and two clusters are obtained for (*S*)-linalool/MBCD complexes (Table 1). After minimization, both of (*R*)- and (*S*)-linalool molecules are located near the wide rim of the MBCD molecule in Orientation-I for all complex conformations, as shown in Figures 8 and 9. The result indicate linalool/MBCD in Orientation-I is the most stable conformation with the lowest $\Delta G = -5.02$, $\Delta E = -43.70$ kcal/mol for (*R*)-linalool/MBCD complex and $\Delta G = -4.98$, $\Delta E = -41.91$ kcal/mol for (*S*)-linalool/MBCD complex, as shown in Tables 1 and 2. The guest molecule cannot go deep down inside the cavity due to the methoxy groups at the C6 position condensing the cavity near the narrow rim of MBCD. Theoretical calculations indicate that MBCD can be used for linalool encapsulation with 1:1 stoichiometry, as shown by the negative complexation energy in Table 2.

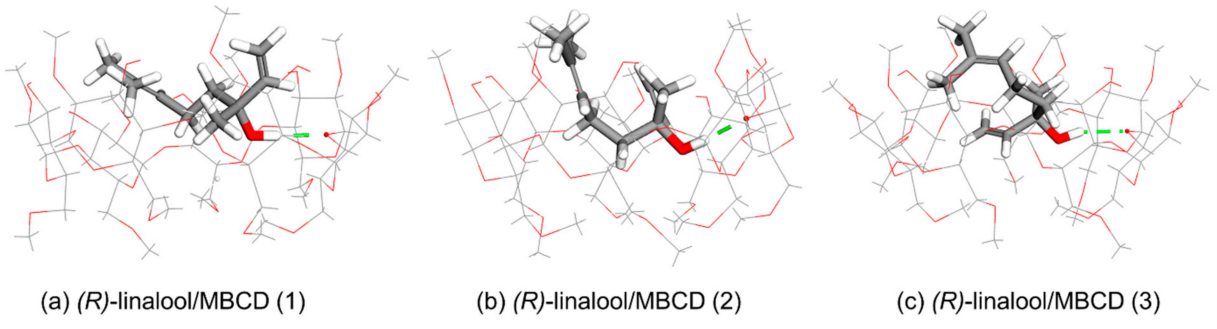

Figure 8. Energy-minimized structure of the 1:1 (*R*)-linalool/MBCD complexes from three clusters using PM7 method. MBCD is presented as a line model. The linalool molecule is presented as a stick model. The green dashed line refers to hydrogen bond.

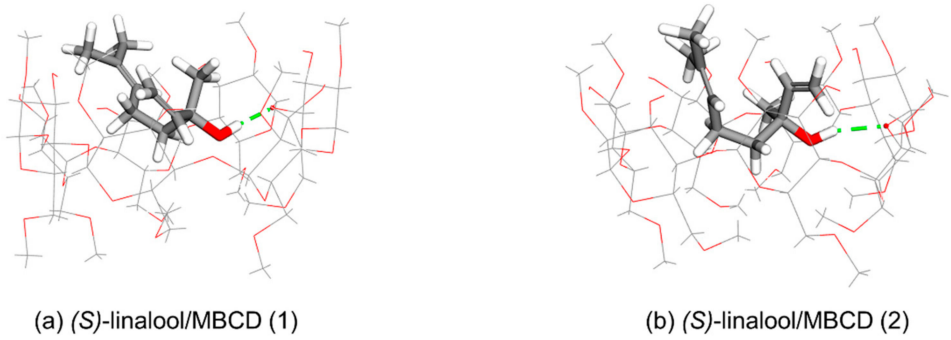

Figure 9. Energy-minimized structure of the 1:1 (*S*)-linalool/MBCD complexes from two clusters using PM7 method. MBCD is presented as a line model. The linalool molecule is presented as a stick model. The green dashed line refers to hydrogen bond.

3.3. Computational Simulation of Linalool/HPBCD Inclusion Complex

Molecular docking calculations indicate three clusters are possible for both of (*R*)- and (*S*)-linalool inclusion complex with HPBCD (Table 1). The width of the wide rim of HPBCD is expanded due to the existence of a hydroxypropyl group at C2 position of one glucose unit which allocates the aliphatic chain of linalool molecule to be occupied (Figures 10 and 11). Orientation-I is found in (*R*)-linalool/HPBCD and (*S*)-linalool/HPBCD complexes in clusters (1) and cluster (2). The dimethyl groups of linalool enantiomers lined up in parallel next to the hydroxypropyl group of HPBCD in linalool/HPBCD (1) and linalool/HPBCD (2) complexes (Figure 10a,b and Figure 11a,b). The configuration of (*R*)-linalool/HPBCD (3) complex remains in Orientation-I, but the position of the dimethyl groups of linalool is away from the hydroxypropyl group of HPBCD, as shown in Figure 10c. The Orientation-II is only found in (*S*)-linalool/HPBCD (3), shown in Figure 11c, with a low occurrence frequency (5%, Table 1). However, from the negative complexation energy in Table 2, this suggests that HPBCD can be used in the 1:1 stoichiometry to encapsulate linalool. The ΔG and ΔE of either (*R*)-linalool/HPBCD ($\Delta G = -4.36$ and $\Delta E = -49.93$ kcal/mol) or (*S*)-linalool/HPBCD ($\Delta G = -4.37$ and $\Delta E = -43.78$ kcal/mol) also indicate Orientation-I is the most stable conformation.

CDs are truncated-cone molecules with hydrophilic outer surface and a lipophilic central cavity. The intermolecular hydrogen bond, van der Waals, and hydrophobic interactions play important roles in complexation of linalool with CDs. Table 4 presents the distance of the intermolecular hydrogen bonds found in PM7 minimized inclusion complex conformations. Four types of hydrogen bonds are established. The first one, which is often found in inclusion complexes, is between an ether-like anomeric oxygen atom of the host molecule and a hydrogen atom of linalool's hydroxyl group ($O4_{(host)} \cdots H_{(OH-L)}$). The second one is between an oxygen atom of linalool's hydroxyl group and a hydrogen atom of the secondary hydroxyl group at O6 of BCD ($O_{(OH-L)} \cdots H_{(O6H-BCD)}$). This enhances the

stability of the complex systems, as shown in (*R*)-linalool/BCD (1) and (*S*)-linalool/BCD (2), with ΔE of −43.94 and −44.86 kcal/mol, respectively. However, if the system has only the second type of hydrogen bond as in (*R*)-linalool/HPBCD, its ΔE value will only be −37.35 kcal/mol. The third type of hydrogen bond is found only in (*S*)-linalool/BCD (4) between the oxygen atom of secondary hydroxyl group O2 of BCD and a hydrogen atom of linalool's hydroxyl group ($O2_{(BCD)} \cdots H_{(OH-L)}$) with ΔE of −43.67 kcal/mol. The last one is found only in linalool/HPBCD complex cluster (2) between the oxygen atom of primary hydroxyl group O6 of HPBCD and a hydrogen atom of linalool's hydroxyl group ($O6_{(HPBCD)} \cdots H_{(OH-L)}$.) with ΔE of −49.93 and −43.78 kcal/mol for (*R*)-linalool/HPBCD (2) and (*S*)-linalool/HPBCD (2), respectively.

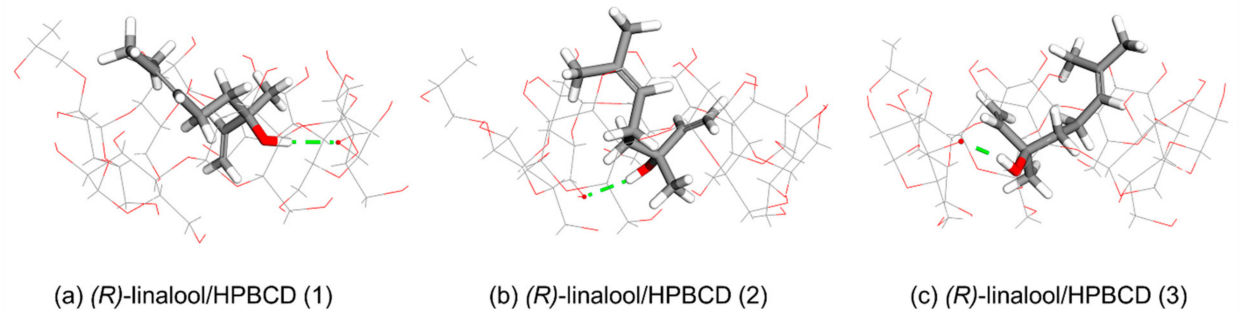

Figure 10. Energy-minimized structure of the 1:1 (*R*)-linalool/HPBCD complexes from three clusters using PM7 method. HPBCD is presented as a line model. The linalool molecule is presented as a stick model. The green dashed line refers to hydrogen bond.

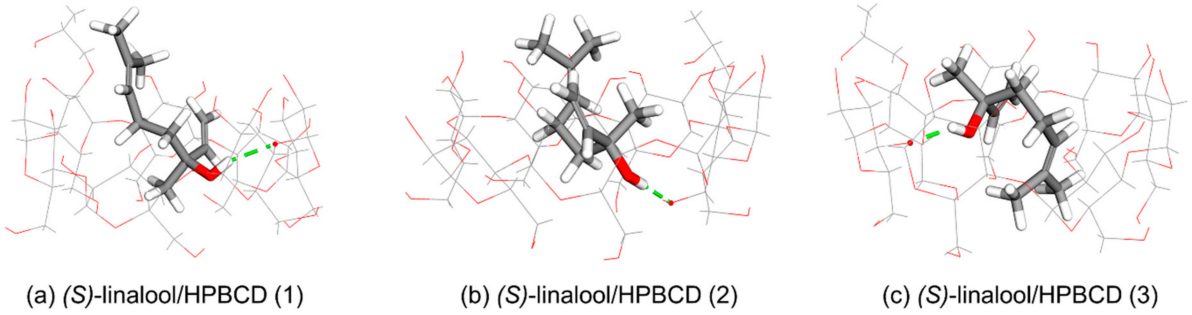

Figure 11. Energy-minimized structure of the 1:1 (*S*)-linalool/HPBCD complexes from three clusters using PM7 method. HPBCD is presented as a line model. The linalool molecule is presented as a stick model. The green dashed line refers to hydrogen bond.

Table 5 presents the summary of molecular docking and semiempirical PM7 calculations of linalool enantiomers inclusion complexed with BCD, MBCD, and HPBCD in 1:1 stoichiometry. The results indicate that BCD, MBCD, and HPBCD and their encapsulation application can be used in enhancing the solubility and stability of linalool enantiomers. The ability to form the complex is confirmed by the complexation energy (ΔE). The more negative ΔE is, the more stable the inclusion complex becomes. The average ΔE values indicate that (*R*)-linalool can form stronger inclusion complexes with all three types of CDs than (*S*)-linalool with the difference between complexation energy of enantiomers 0.41, 1.40, and 2.56 kcal/mol for BCD, MBCD, and HPBCD, respectively (Table 5). The enantiomeric selection occurs due to the chirality of CD molecules. The structures of BCDs consist of 7 d-glucose (dextrose) units, which have four chiral carbons per unit. The stereochemistry at each chiral carbon can be labelled as R or S; in this way, carbons 2 through 5 in dextrose could be labeled 2R, 3S, 4R, 5R. This might be the reason why (*R*)-linalool can form a touch stable inclusion complex with BCD it his study.

Table 4. The complexation energy (Δ*E*, in kcal/mol) and the distance of hydrogen bonds between linalool molecules (L) and three different CDs (BCD, MBCD, and HPBCD) molecules, obtained from PM7 minimized inclusion complex structures.

Inclusion Complex	Cluster	Δ*E*		Distance (Å)
(*R*)-linalool/BCD	(1)	−43.94	$O4_{(BCD)} \cdots H_{(OH-L)}$	2.12
			$O_{(OH-L)} \cdots H_{(O6H-BCD)}$	1.94
	(2)	−40.71	$O4_{(BCD)} \cdots H_{(OH-L)}$	1.97
	(3)	−41.84	$O4_{(BCD)} \cdots H_{(OH-L)}$	2.05
	(4)	−37.82	$O4_{(BCD)} \cdots H_{(OH-L)}$	2.25
(*S*)-linalool/BCD	(1)	−39.46	$O4_{(BCD)} \cdots H_{(OH-L)}$	2.21
	(2)	−44.86	$O4_{(BCD)} \cdots H_{(OH-L)}$	2.09
			$O_{(OH-L)} \cdots H_{(O6H-BCD)}$	1.84
	(3)	−41.75	$O4_{(BCD)} \cdots H_{(OH-L)}$	1.98
	(4)	−43.67	$O2_{(BCD)} \cdots H_{(OH-L)}$	1.96
(*R*)-linalool/MBCD	(1)	−43.42	$O4_{(MBCD)} \cdots H_{(OH-L)}$	1.98
	(2)	−43.70	$O4_{(MBCD)} \cdots H_{(OH-L)}$	1.98
	(3)	−37.94	$O4_{(MBCD)} \cdots H_{(OH-L)}$	2.08
(*S*)-linalool/MBCD	(1)	−41.91	$O4_{(MBCD)} \cdots H_{(OH-L)}$	2.03
	(2)	−41.23	$O4_{(MBCD)} \cdots H_{(OH-L)}$	2.07
(*R*)-linalool/HPBCD	(1)	−43.59	$O4_{(HPBCD)} \cdots H_{(OH-L)}$	2.10
	(2)	−49.93	$O6_{(HPBCD)} \cdots H_{(OH-L)}$	2.12
	(3)	−37.35	$O_{(OH-L)} \cdots H_{(O6H-HPBCD)}$	1.01
(*S*)-linalool/HPBCD	(1)	−41.59	$O4_{(HPBCD)} \cdots H_{(OH-L)}$	2.16
	(2)	−43.78	$O6_{(HPBCD)} \cdots H_{(OH-L)}$	2.01
	(3)	−42.95	$O4_{(HPBCD)} \cdots H_{(OH-L)}$	1.99

Table 5. The percent frequency occurs in docking calculation, the complexation energy (Δ*E*) of each inclusion complexes cluster, the average complexation energy values of enantiomeric linalool/BCD complexes, and the difference between complexation energy of (*R*)- and (*S*)-enantiomers (Δ enantiomers) using PM7 calculations.

Inclusion Complex	Cluster	Frequency (%)	Δ*E* (kcal/mol)		
			Δ*E*	Average	Δ Enantiomers
(*R*)-linalool/BCD	(1)	64	−43.94	−42.67	0.41
	(2)	31	−40.71		
	(3)	1	−41.84		
	(4)	4	−37.82		
(*S*)-linalool/BCD	(1)	41	−39.46	−42.26	
	(2)	46	−44.86		
	(3)	12	−41.75		
	(4)	1	−43.67		
(*R*)-linalool/MBCD	(1)	90	−43.42	−43.22	1.40
	(2)	6	−43.70		
	(3)	4	−37.94		
(*S*)-linalool/MBCD	(1)	87	−41.91	−41.82	
	(2)	13	−41.23		
(*R*)-linalool/HPBCD	(1)	69	−43.59	−44.42	2.56
	(2)	22	−49.93		
	(3)	9	−37.35		
(*S*)-linalool/HPBCD	(1)	86	−41.59	−41.86	
	(2)	9	−43.78		
	(3)	5	−42.95		

3.4. Phase Solubility Study of Linalool/CD Inclusion Complexes

Phase solubility study was conducted to evaluate the change in linalool aqueous solubility after being encapsulated by CDs. The amount of dissolved linalool in the CD solutions of various concentrations was quantified by HPLC. Figure 12 shows the concentration of dissolved linalool versus the concentration of each CD solution. The concentration profile of linalool encapsulated with BCD in Figure 12a is comparable to B-type diagram from Higuchi and Connors' types of phase solubility. B-type diagram which exhibits an initial linear growth followed by a plateau indicates the formation of complexes which limit further aqueous solubility improvement [26]. The initial linear region shows that linalool solubility increases with increasing concentration of BCD. However, at a higher concentration of BCD, linalool solubility becomes constant. This region implies the precipitation of the linalool/BCD inclusion complexes. The precipitation is likely caused by BCD's low aqueous solubility and its tendency to self-assemble in aqueous solutions [14]. In Figure 12b,c, the concentration of linalool linearly increases with increasing concentration of MBCD and HPBCD. The aqueous solubility of linalool can thus be enhanced by varying the concentrations of the host molecules. In this case, MBCD and HPBCD are more effective in increasing the aqueous solubility of linalool in the form of inclusion complexes mainly due to their higher aqueous solubility compared to BCD.

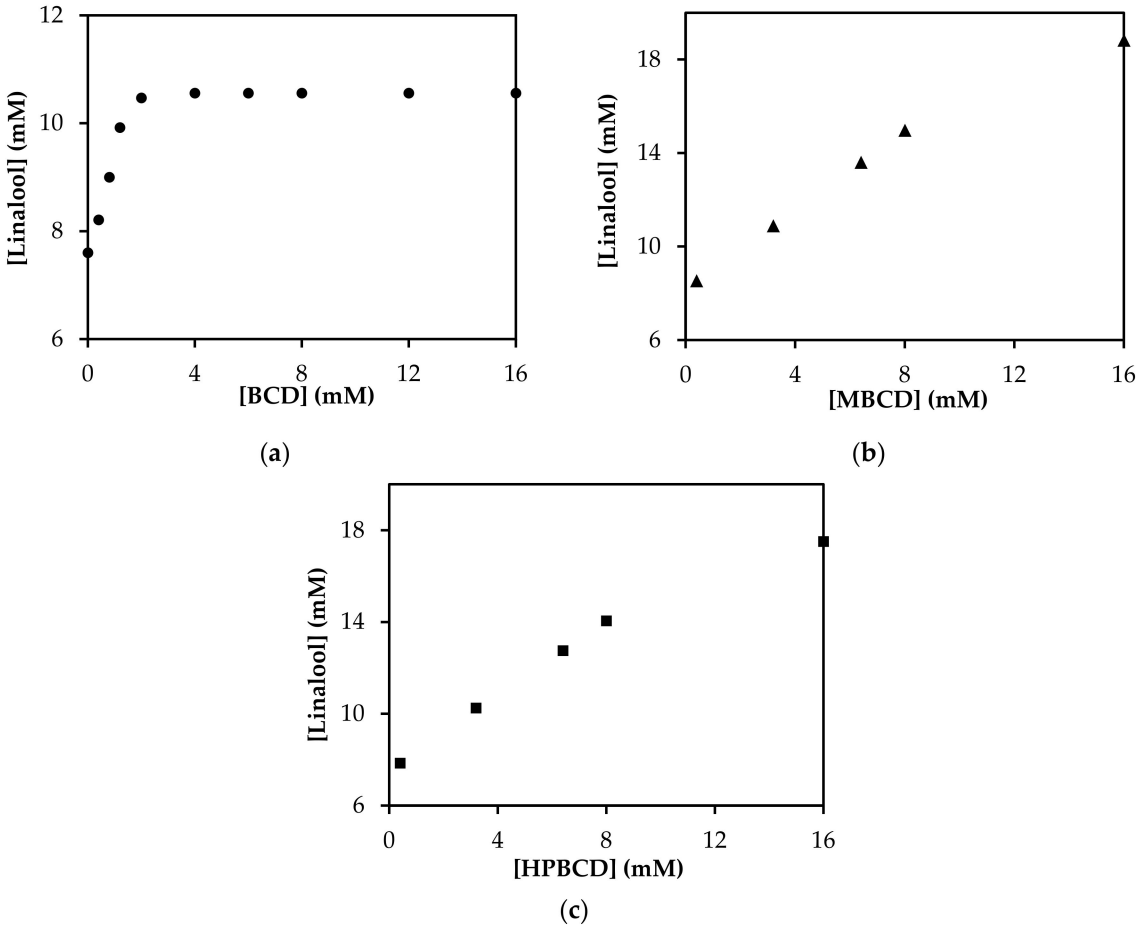

Figure 12. Phase solubility diagrams of (**a**) linalool in BCD solution, (**b**) linalool in MBCD solution, and (**c**) linalool in HPBCD solution.

3.5. Solvent Effect on the Encapsulation Efficiency of Linalool/CD Inclusion Complexes

In this study, the inclusion complexes were prepared in CD solutions dissolved ethanol-water solvent. To obtain the highest encapsulation efficiency of each CD, the optimal concentration of ethanol as a co-solvent was evaluated. The amount of linalool in inclusion

complexes prepared in solvents of different ethanol concentrations was quantified by HPLC. The encapsulation efficiency of each CD was calculated using Equation (2). The results show that ethanol content in the solvent affects the encapsulation efficiency. For BCD, the optimal ethanol concentration is 30 vol% which produces an encapsulation efficiency of 66.30%, as shown in Figure 13a. Solvents with more than 30 vol% ethanol limit the solubility of BCD which led to precipitate formation [27]. For MBCD and HPBCD, the encapsulation efficiency is positively correlated with ethanol concentration, as shown in Figure 13b,c. The highest encapsulation efficiencies for MBCD and HPBCD are 51.38% and 32.31%, respectively. From these results, 30 vol% ethanol was used in linalool/BCD inclusion complex preparation, and 80 vol% ethanol was used for linalool/MBCD and linalool/HPBCD inclusion complex preparation for further characterization analyses.

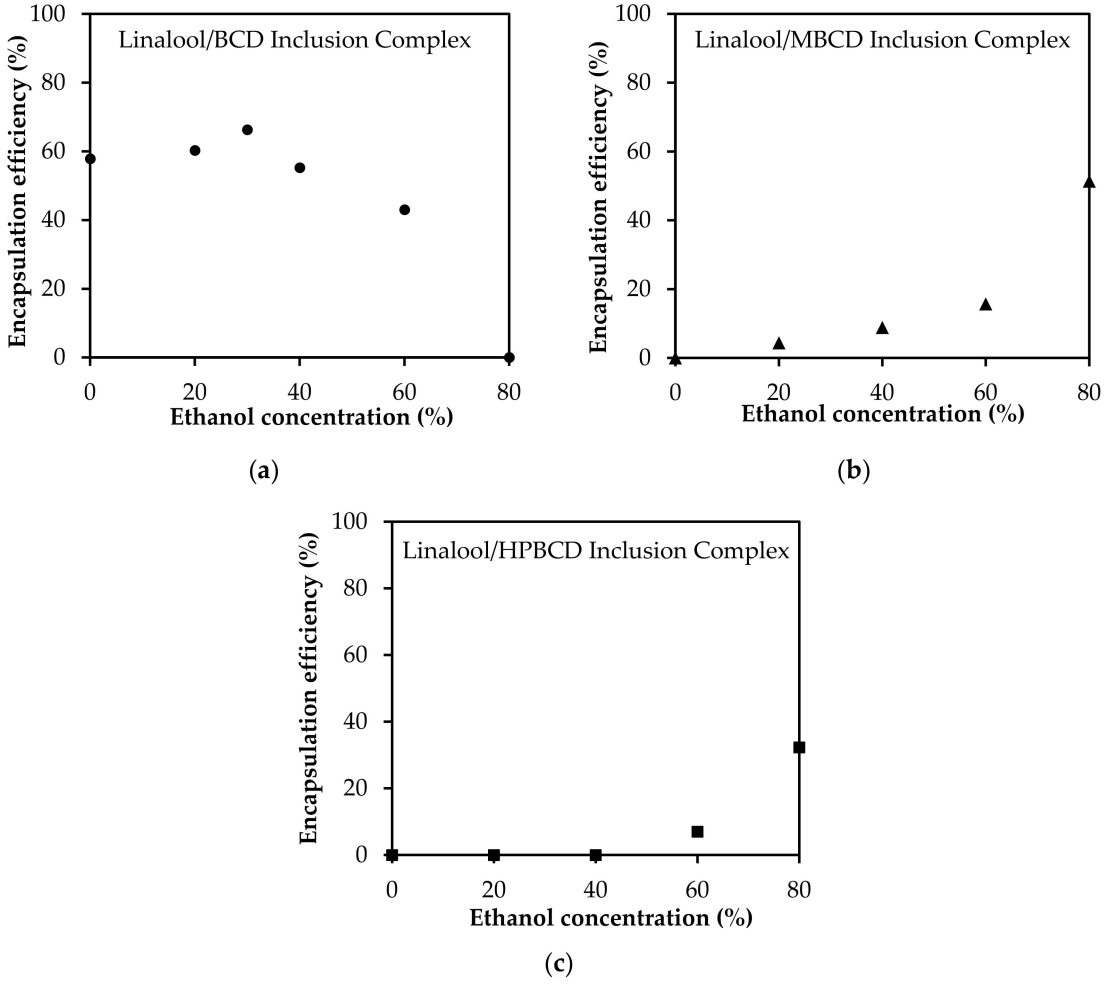

Figure 13. The effect of ethanol content on the encapsulation efficiency of (**a**) linalool/BCD inclusion complex, (**b**) linalool/MBCD inclusion complex, and (**c**) linalool/HPBCD inclusion complex.

3.6. Characterization of Linalool/CD Inclusion Complexes by FTIR

FTIR spectrometer was used to investigate the functional groups of the inclusion complexes compared to the pure compounds in order to confirm inclusion complex formation. Figure 14 illustrates the FTIR spectra of pure linalool, pure CDs, and the inclusion complexes. Linalool/BCD inclusion complex exhibits a slight peak shift from 3340 to 3378 cm^{-1}. Linalool/MBCD inclusion complex exhibits a slight shift in peaks from 3404 to 3427 cm^{-1} and from 1030 to 1043 cm^{-1}. Linalool/HPBCD inclusion complex exhibits a slight shift in peaks from 3408 to 3425 cm^{-1} and from 1030 to 1035 cm^{-1}. All of the inclusion complex spectra exhibit a slight peak shift at ~3400 cm^{-1} which corresponds to

O–H stretching vibration, while the peak shifts at ~1000 cm^{-1} observed in linalool/MBCD and linalool/HPBCD inclusion complexes correspond to C–O stretching vibration. These peak shifts in O–H and C–O stretching vibration imply bond formations between the CDs and linalool. In all inclusion complex spectra, a clear peak is observed at ~2900 cm^{-1} which indicates the combination of linalool and the CDs. Many characteristic peaks from pure linalool are also absent in the inclusion complex spectra, possibly due to the encapsulation of linalool inside the CD cavity. These FTIR results which show bond formations between linalool and the CDs as well as the lack of some linalool characteristic peaks serve as evidence of complex formation.

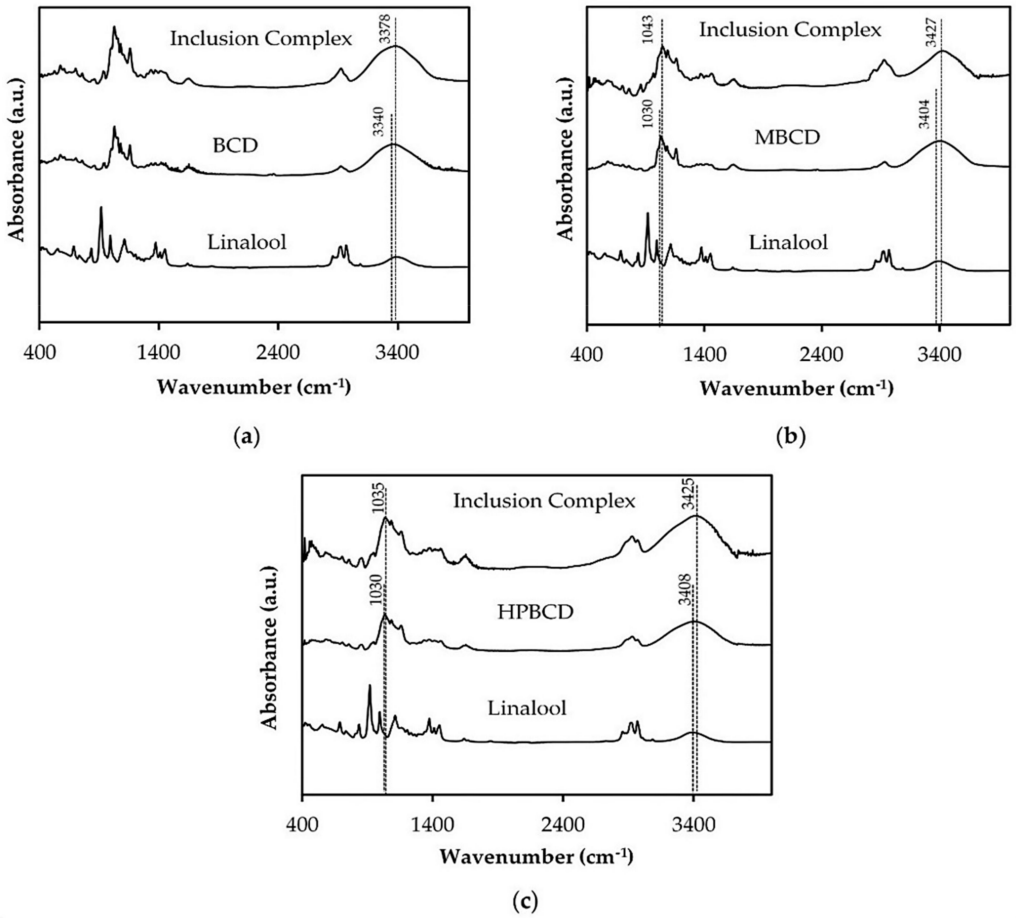

Figure 14. The FTIR spectra of (**a**) linalool/BCD inclusion complex, BCD, and linalool, (**b**) linalool/MBCD inclusion complex, MBCD, and linalool, and (**c**) linalool/HPBCD inclusion complex, HPBCD, and linalool.

3.7. Characterization of Linalool/CD Inclusion Complexes by TGA

Thermal analysis was performed with TGA to investigate the stability of linalool/CD inclusion complexes compared to the pure compounds. Figure 15 illustrates the TG and DTG curves which show the mass percentage and the rate of mass loss of the inclusion complexes, pure CDs, and pure linalool. Pure CDs show the mass loss from moisture content at temperatures between 60 and 110 °C and from thermal decompositions of BCD, MBCD, and HPBCD at temperatures of 330, 370, and 350 °C, respectively. For pure linalool, the mass loss from linalool volatilization is observed in the temperature range of 100 to 190 °C. The TG and DTG curves of all inclusion complexes show mass loss from moisture content and thermal decomposition of CDs without substantial mass loss due to linalool volatilization. Hence, TGA analysis showed an increase in the thermostability of linalool after being encapsulated by CDs which confirmed the inclusion complex formation.

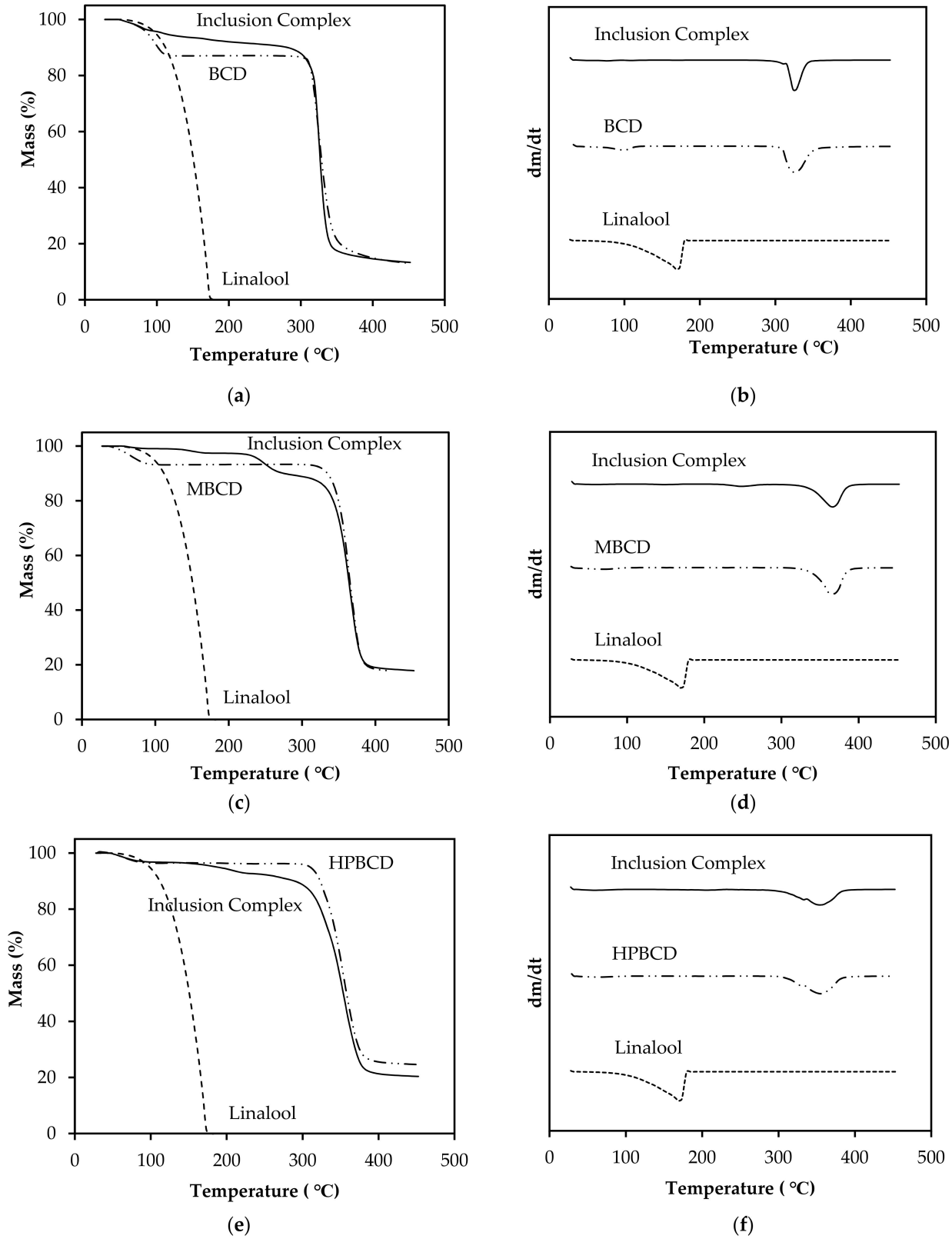

Figure 15. TG and DTG curves of (**a**,**b**) linalool/BCD inclusion complex, BCD, and linalool; (**c**,**d**) linalool/MBCD inclusion complex, MBCD, and linalool; (**e**,**f**) linalool/HPBCD inclusion complex, HPBCD, and linalool.

3.7.1. Characterization of Linalool/CD Inclusion Complexes by DSC

DSC was used for an investigation of heat flow into or out of the inclusion complexes and the pure compounds with increasing temperature to further confirm inclusion complex formation. The DSC curves of linalool/CD inclusion complexes, pure CDs, and pure linalool are shown in Figure 16. For all CDs, the results show a broad endothermic peak between 60 and 120 °C from the energy change due to moisture loss. Pure linalool exhibits an endothermic peak at ~200 °C which corresponds to linalool volatilization. However, all inclusion complexes show only a broad endothermic peak due to the energy change from moisture loss without linalool volatilization. The lack of a heat flow peak corresponding to linalool volatilization further confirms the inclusion complex formation between linalool and the CDs. Therefore, the characterization results from FTIR, TGA, and DSC confirm the formation of linalool/BCD, linalool/MBCD, and linalool/HPBCD inclusion complexes in this experimental study.

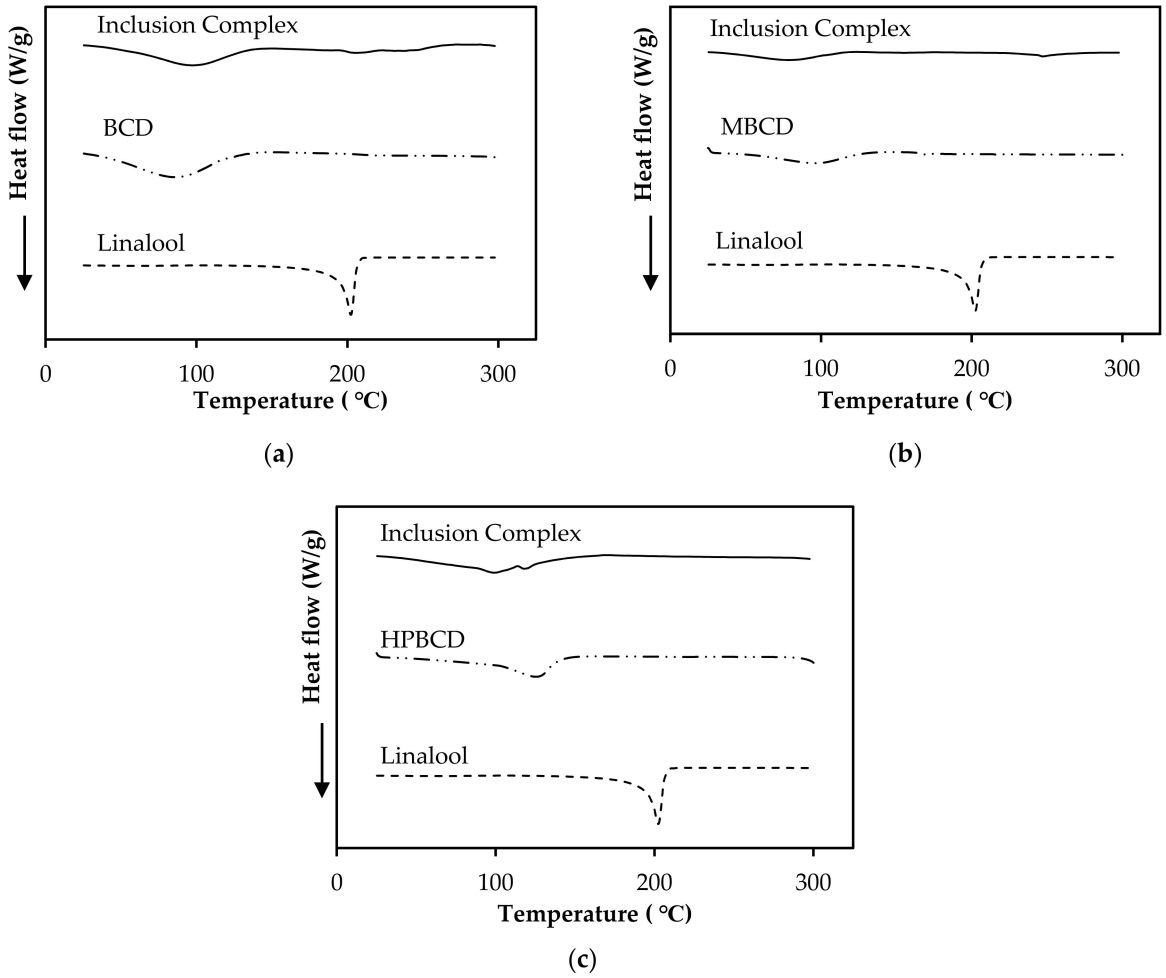

Figure 16. DSC curves of (**a**) linalool/BCD inclusion complex, BCD, and linalool; (**b**) linalool/MBCD inclusion complex, MBCD, and linalool; (**c**) linalool/HPBCD inclusion complex, HPBCD, and linalool.

3.7.2. Preservation Study of Linalool/CD Inclusion Complexes

The preservation of linalool in the form of linalool/CD inclusion complexes was evaluated to investigate the improvement of linalool stability after being encapsulated by CDs. The remaining amount of linalool in the inclusion complexes at the storage temperature of 25 °C was quantified every 7 days and compared to pure linalool as shown in Figure 17.

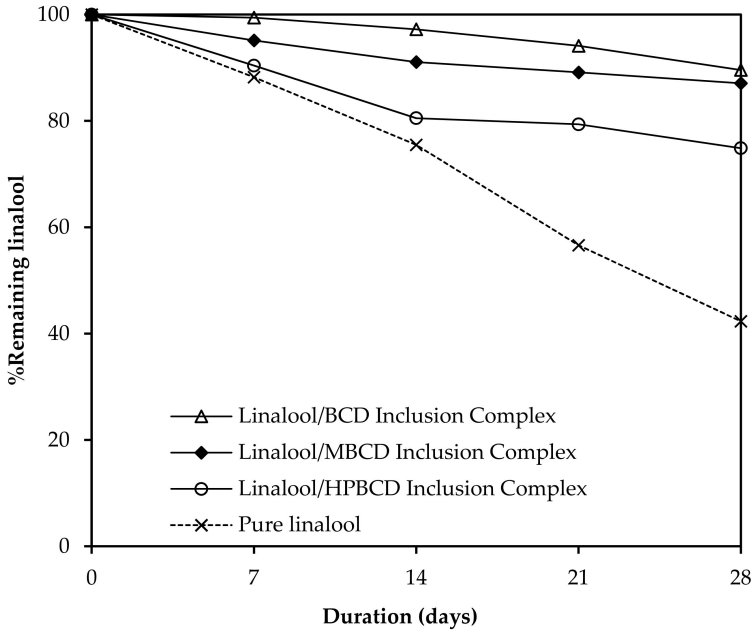

Figure 17. Stability curves of linalool/CD inclusion complexes and pure linalool.

The percentage of remaining linalool was calculated using Equation (3). After 28-day storage in air, only 42.30% of pure linalool remained. For the inclusion complexes, 89.57%, 87.07%, and 74.86% of linalool remained from linalool/BCD, linalool/MBCD, and linalool/HPBCD, respectively. From the increase in the percentage of remaining linalool in inclusion complexes, encapsulation technique with CDs can be used to stabilize and preserve linalool. Note here that the percentages of remaining linalool in linalool/MBCD and linalool/HPBCD inclusion complexes are lower than that of linalool/BCD inclusion complex. Since MBCD and HPBCD have high aqueous solubility, the moisture in air may cause dissolution of both MBCD and HPBCD, allowing the encapsulated linalool to be released. Linalool/BCD inclusion complex is thus the most stable host molecule due to its low aqueous solubility.

3.7.3. Enantiomeric Selection of Linalool/CD Inclusion Complexes

This study also focused on the enantiomeric selectivity of CDs in encapsulating the enantiomers of racemic linalool standard. The extracted linalool from solid inclusion complexes was analyzed by GC-FID equipped with a chiral column. The enantiomeric selectivity of encapsulated linalool compared to the racemic standard is shown in Table 6. The percentages of (*R*)-linalool in all the inclusion complexes are higher than that in the racemic linalool standard, with linalool/BCD showing the largest increase of ~10%. This result shows that CD host molecules have higher enantiomeric selectivity toward (*R*)-linalool. Since the change in linalool enantiomer ratio can cause a considerable change in taste and odor, the results from this study can be used to enhance the overall quality of linalool-containing products. Other factors may be varied in further studies to improve the linalool enantiomeric selectivity of CDs.

Table 6. Enantiomeric selection of linalool by CDs.

Inclusion Complex	%Enantiomer in the Inclusion Complexes	
	(*R*)-Linalool	(*S*)-Linalool
Racemic linalool (standard)	49.50 ± 0.16	50.50 ± 0.16
Linalool/BCD	54.53 ± 0.34	44.62 ± 0.34
Linalool/MBCD	52.49 ± 0.20	47.51 ± 0.20
Linalool/HPBCD	51.51 ± 0.10	48.49 ± 0.10

4. Conclusions

This study investigated encapsulation of linalool with CDs, which are BCD, MBCD, and HPBCD. A computational simulation was utilized to investigate the conformations and the binding energy between the enantiomers of linalool and all CDs in the inclusion complexes. The inclusion complexes were prepared using 1:1 host-guest molar ratio of linalool and CDs based on the computer simulation result. The phase solubility study shows an enhancement in aqueous solubility of linalool after being encapsulated by CDs. Due to higher aqueous solubility of MBCD and HPBCD, they are more effective in increasing the aqueous solubility of the encapsulated linalool. From the stability test, all CDs are able to stabilize and preserve linalool in the form of inclusion complexes. However, due to low aqueous solubility of BCD, it is the most effective CD in preserving linalool. The amount of remaining linalool is increased from 42.30% in pure linalool to 89.57% in the linalool/BCD inclusion complex. Moreover, all CDs exhibit enantiomeric selectivity to (*R*)-linalool. BCD shows the highest enantiomeric selectivity which corresponds with the computational simulation results showing that (*R*)-linalool form a more stable inclusion complex with BCD. Therefore, nanoencapsulation of linalool with CDs in the form of inclusion complexes improves the aqueous solubility and the stability of linalool which can lead to longer shelf life and better distribution of linalool in water-based products. BCD is the most suitable host molecule to encapsulate linalool due to its cost, enantiomeric selectivity and preservation ability.

Author Contributions: Data curation, T.P.; Investigation, T.P., L.L. and P.T.; Methodology, T.P., S.K. and K.J.; Project administration, L.L. and P.T.; Supervision, L.L. and P.T.; Writing—original draft, T.P., S.K., K.J., L.L. and P.T.; Writing—review & editing, L.L. and P.T. All authors have read and agreed to the published version of the manuscript.

Funding: This research received no external funding.

Institutional Review Board Statement: Not applicable.

Informed Consent Statement: Not applicable.

Data Availability Statement: Not applicable.

Acknowledgments: This study was supported by Thammasat University Research Fund, Contract No. TUFT 068/2563 and the scholarship for the Excellent Thai Student of Sirindhorn International Institute of Technology. The authors appreciatively acknowledge the Center of Scientific Equipment for Advanced Research, Thammasat University (TUCSEAR) for access to the analytical instruments.

Conflicts of Interest: The authors declare no conflict of interest.

References

1. Mughal, M.H. Linalool: A Mechanistic Treatise. *J. Nutr. Food Technol.* **2019**, *2*, 1–5. [CrossRef]
2. Turek, C.; Stintzing, F.C. Stability of Essential Oils: A Review. *Compr. Rev. Food Sci. Food Saf.* **2013**, *12*, 40–53. [CrossRef]
3. Lara, C.S.; Barata, L.E.S.; Sampaio, P.d.T.B.; Eberlin, M.N.; Fidelis, C.H.d.V. Linalool Enantiomeric Distribution in Rosewood-reminiscent Populations in Central Amazon. *J. Essent. Oil Res.* **2018**, *30*, 464–469. [CrossRef]
4. Padrayuttawat, A.; Yoshizawa, T.; Tamura, H.; Tokunaga, T. Optical Isomers and Odor Thresholds of Volatile Constituents in Citrus Sudachi. *J. Food Sci. Technol. Int.* **1997**, *3*, 402–408. [CrossRef]
5. Aprotosoaie, A.C.; Hăncianu, M.; Costache, I.I.; Miron, A. Linalool: A Review on a Key Odorant Molecule with Valuable Biological Properties. *Flavour Frag. J.* **2014**, *29*, 193–219. [CrossRef]
6. Bonnländer, B.; Cappuccio, R.; Liverani, F.S.; Winterhalter, P.J.F. Analysis of Enantiomeric Linalool Ratio in Green and Roasted Coffee. *Flavour Frag. J.* **2006**, *21*, 637–641. [CrossRef]
7. Jambhekar, S.S.; Breen, P. Cyclodextrins in Pharmaceutical Formulations I: Structure and Physicochemical Properties, Formation of Complexes, and Types of Complex. *Drug Discov. Today* **2016**, *21*, 356–362. [CrossRef]
8. Marques, H.M.C. A Review on Cyclodextrin Encapsulation of Essential Oils and Volatiles. *Flavour Frag. J.* **2010**, *25*, 313–326. [CrossRef]
9. Pinho, E.; Grootveld, M.; Soares, G.; Henriques, M. Cyclodextrins as Encapsulation Agents for Plant Bioactive Compounds. *Carbohydr. Polym.* **2014**, *101*, 121–135. [CrossRef]
10. Mura, P. Analytical Techniques for Characterization of Cyclodextrin Complexes in Aqueous Solution: A Review. *J. Pharm. Biomed. Anal.* **2014**, *101*, 238–250. [CrossRef]

11. Gingter, S.; Bezdushna, E.; Ritter, H. Chiral Recognition of Macromolecules with Cyclodextrins: pH-and Thermosensitive Copolymers from N-isopropylacrylamide and N-acryloyl-D/L-phenylalanine and Their Inclusion Complexes with Cyclodextrins. *Beilstein J. Org. Chem.* **2011**, *7*, 204–209. [CrossRef]
12. Lee, J.-u.; Lee, S.-S.; Lee, S.; Oh, H.B. Noncovalent Complexes of Cyclodextrin with Small Organic Molecules: Applications and Insights into Host–Guest Interactions in the Gas Phase and Condensed Phase. *Molecules* **2020**, *25*, 4048. [CrossRef] [PubMed]
13. Capelezzo, A.P.; Mohr, L.C.; Dalcanton, F.; de Mello, J.M.M.; Fiori, M.A. β-Cyclodextrins as Encapsulating Agents of Essential Oils. *Cyclodext.-A Versatile Ingred. IntechOpen* **2018**, 169–200.
14. Saokham, P.; Muankaew, C.; Jansook, P.; Loftsson, T. Solubility of Cyclodextrins and Drug/cyclodextrin Complexes. *Molecules* **2018**, *23*, 1161. [CrossRef]
15. Abril-Sánchez, C.; Matencio, A.; Navarro-Orcajada, S.; García-Carmona, F.; López-Nicolás, J.M. Evaluation of the properties of the essential oil citronellal nanoencapsulated by cyclodextrins. *Chem. Phys. Lipids.* **2019**, *219*, 72–78. [CrossRef]
16. Biovia, D.S. *Discovery Studio Visualizer*; Dassault Systèmes: San Diego, CA, USA, 2017.
17. Steiner, T.; Koellner, G. Crystalline Beta-cyclodextrin Hydrate at Various Humidities: Fast, Continuous, and Reversible Dehydration Studied by X-ray Diffraction. *J. Am. Chem. Soc.* **1994**, *116*, 5122–5128. [CrossRef]
18. Aree, T.; Hoier, H.; Schulz, B.; Reck, G.; Saenger, W. Novel Type of Thermostable Channel Clathrate Hydrate Formed by Heptakis (2, 6-di-O-methyl)-β-cyclodextrin· 15 H_2O—A Paradigm of the Hydrophobic Effect. *Angew. Chem. Int. Ed.* **2000**, *39*, 897–899. [CrossRef]
19. Harata, K.; Rao, C.T.; Pitha, J.; Fukunaga, K.; Uekama, K. Crystal Structure of 2-O-[(S)-2-hydroxypropyl] Cyclomaltoheptaose. *Carbohydr. Res.* **1991**, *222*, 37–45. [CrossRef]
20. Frisch, M.; Trucks, G.; Schlegel, H.; Scuseria, G.; Robb, M.; Cheeseman, J.; Scalmani, G.; Barone, V.; Petersson, G.; Nakatsuji, H. *Gaussian16, RevisionB. 01*; Gaussian, Inc.: Wallingford, CT, USA, 2016.
21. Morris, G.M.; Huey, R.; Lindstrom, W.; Sanner, M.F.; Belew, R.K.; Goodsell, D.S.; Olson, A.J. AutoDock4 and AutoDockTools4: Automated Docking with Selective Receptor Flexibility. *J. Comput. Chem.* **2009**, *30*, 2785–2791. [CrossRef]
22. Ceborska, M. Structural Investigation of the β-cyclodextrin Complexes with Linalool and Isopinocampheol–Influence of Monoterpenes Cyclicity on the Host–guest Stoichiometry. *Chem. Phys. Lett.* **2016**, *651*, 192–197. [CrossRef]
23. Case, D.A.; Belfon, H.M.A.K.; Ben-Shalom, I.Y.; Brozell, S.R.; Cerutti, D.S.; Cheatham, T.E., III; Cruzeiro, V.W.D.; Duke, G.; Giambasu, M.K.; Gilson, H.; et al. *Amber 2021*; University of California: San Francisco, CA, USA, 2021.
24. Kirschner, K.N.; Yongye, A.B.; Tschampel, S.M.; González-Outeiriño, J.; Daniels, C.R.; Foley, B.L.; Woods, R.J. GLYCAM06: A Generalizable Biomolecular Force Field. Carbohydrates. *J. Comput. Chem.* **2008**, *29*, 622–655. [CrossRef] [PubMed]
25. Sinlikhitkul, N.; Toochinda, P.; Lawtrakul, L.; Kuropakornpong, P.; Itharat, A. Encapsulation of Plumbagin Using Cyclodextrins to Enhance Plumbagin Stability: Computational Simulation, Preparation, Characterization, and Application. *J. Incl. Phenom. Macrocycl. Chem.* **2019**, *93*, 229–243. [CrossRef]
26. Connors, K.; Higuchi, T. Phase Solubility Techniques. *Adv. Anal. Chem. Instrum.* **1965**, *4*, 117–122.
27. Chatjigakis, A.K.; Donze, C.; Coleman, A.W.; Cardot, P. Solubility Behavior of Beta-cyclodextrin in Water/cosolvent Mixtures. *Anal. Chem.* **1992**, *64*, 1632–1634. [CrossRef]